

## Article

# Correlation between the Material System and the Magnetic Properties in Thermoset-Based Multipolar Ring Magnets

Uta Rösel \*  and Dietmar Drummer

Institute of Polymer Technology, Friedrich-Alexander-Universität Erlangen-Nürnberg, 91058 Erlangen, Germany

\* Correspondence: uta.ur.roesel@fau.de

**Abstract:** Multipolar bonded magnets based on thermosets offer the opportunity to expand the applications of bonded magnets with respect to an increasing chemical and thermal resistance compared to thermoplastics. To utilise this option, the correlation between the material system and the magnetic properties must be explored amongst other influencing factors. This paper investigates the magnetic properties and the orientation of thermoset- (epoxy resin and phenolic resin) based bonded ring magnets with a hard magnetic filler of strontium-ferrite-oxide. The influence of the matrix material and the filler grade on the magnetic properties is correlated with the material characterisation showing a high impact of the embedding of the fillers into the matrix on the orientation and with that the magnetic properties. Based on a network theory, it can be justified that the magnetic properties can be increased due to a phenolic resin and a high filler grade. Further, it was shown that the orientation along the sample depth is highly affected by the strength of the outer magnetic field and limited in terms of the high-tool temperature in a thermoset-based production. With that, the sample depth, which reveals a proper orientation, is restricted so far.

**Keywords:** hard magnetic filler; highly filled thermosets; polymer bonded magnets; multipolar magnets; network theory



**Citation:** Rösel, U.; Drummer, D. Correlation between the Material System and the Magnetic Properties in Thermoset-Based Multipolar Ring Magnets. *Magnetism* **2023**, *3*, 226–244. <https://doi.org/10.3390/magnetism3030018>

Academic Editor: Pablo Guardia

Received: 14 February 2023

Revised: 24 May 2023

Accepted: 26 July 2023

Published: 14 August 2023



**Copyright:** © 2023 by the authors. Licensee MDPI, Basel, Switzerland. This article is an open access article distributed under the terms and conditions of the Creative Commons Attribution (CC BY) license (<https://creativecommons.org/licenses/by/4.0/>).

## 1. Introduction

Polymer bonded magnets mainly exist as two material groups—the matrix material and the hard magnetic filler. The matrix material currently defines the production process, where thermoplastic-based bonded magnets are mainly fabricated by injection moulding and thermoset-based bonded magnets by pressing [1]. This highly effects the possible application properties, where, for example, the filler grade can reach up to 85 vol.-% in pressed magnets with higher magnetic properties compared to magnets fabricated by injection moulding. The thermoplastic-based bonded magnets reveal, on the other hand, a high freedom of design [2], size accuracy [3] and a possible functional integration [4], but a lack in magnetic properties due to the limitation of the filler grade by 60 vol.-% [3]. The limitation of filler grade in the injection-moulding process goes along with the increase of the viscosity. In thermoplastic-based bonded magnets, high viscosity and the temperature setting within the process lead to a fast cooling outer phase, where a significant lack of orientation can be seen [5]. This reduces the magnetic properties on the outer surface of the magnets, which is important in terms of sensor applications, for example. Beside applications in the field of sensors, polymer bonded magnets are used in driving applications, mainly in terms of a magnetic excitation of synchronous or direct current (DC) machines [6]. However, the demand for the freedom of design within these applications allows fabrication only via injection moulding, and with that a thermoplastic-based matrix material has to be used. However, the limitation of the filler grade, the reduction of the orientation in the outer surface, and a general lack of temperature and media resistance in thermoplastics hinder the usage of polymer-bonded magnets in drive applications. This can be seen in the fields of chemical industry or cooling water pumps, for example. Therefore, the possible application

for polymer-bonded magnets could be expanded significantly if they could be fabricated based on thermosets instead of thermoplastics in the injection-moulding process. So far, polymer-bonded magnets based on thermosets are mainly fabricated by pressing. This leads to a significant lack of design freedom compared to the injection-moulding process. Further, an orientation of the fillers and the usage of the material potential of anisotropic fillers is highly limited in pressed magnets. With that, the demand for possible application cannot be realised by polymer-bonded magnets based on thermosets and fabricated by pressing. The high degree of freedom in the geometry and the magnetisation structure as well as the integrated orientation and magnetisation process in the fabrication process can only be reached by the injection-moulding process.

### *1.1. Flow Behaviour and Reaction Kinetics of Filled Thermoset Systems*

Thus far, the impact of fillers within thermosets has been investigated in different papers with respect to the flow behaviour and the reaction kinetics [7–10]. For example, Ref. [11] states that fillers affect the curing process in the change of the thermal conductivity within epoxy resins (EP). In [12], the increase of free energy in fillers when applied in the material system was proven, which enables the gelation to be realised more readily. Ref. [13] proved that thermal conductivity increases with filler content, as shown in [11], and further builds a mesh work with a filler grade of more than 50 vol.-%. Further, cuboid particles and a great particle size increase the impact of fillers on thermal conductivity [13]. According to [14], flow behaviour can be improved by small filler grades and high filler sizes, but the cycle time is reduced by higher filler grades and smaller particles. Ref. [15] defines the gelation as a function of the molecular network, which results in a high impact of the adhesive properties of the particles on the behaviour of the fillers in the network. With respect to this, Ref. [15] compares two stadiums of the integration, one with a high adhesive force between the fillers and the network and one with no adhesive force. This general research of the effect of fillers within thermosets and the impact on the flow and curing behaviour is mainly based on a small filler grade of less than 10 wt.-%. Transferring results to the behaviour of hard magnetic fillers in thermosets with a filler grade up to 90 wt.-% is not possible.

To enable the usage of thermosets within polymer-bonded magnets in the injection-moulding fabrication, the impact of hard magnetic fillers on the flow and curing process must be known. First attempts were executed by [16], amongst others, but these processes reveal a certain lack of systematic investigation. Ref. [17] defined several factors which influence the flow and curing process in highly filled thermoset-based systems in an epoxy resin and showed that the hard magnetic filler type strontium-ferrite-oxide (SrFeO) is more likely to act like an adhesive filler in a network, whereas neodymium-iron-boron (NdFeB) is more likely to behave like a non-adhesive filler according to [15]. In [18], this general behaviour of hard magnetic fillers in thermosets was extended by correlating the material properties with the magnetic and mechanical properties. It was further shown that SrFeO is integrated within the network by building adhesive forces, but the integration grade differs in terms of the chosen matrix material. As shown in Figure 1, SrFeO in EP-based material systems is more integrated with less space in the filler within the network compared to phenolic resin (PF)-based systems.

With that, first attempts at observing the impact of hard magnetic fillers in highly filled thermosets on the flow and curing process are realised. The investigations in [17,18] primarily enable the use of thermoset-based bonded magnets in the injection-moulding process as a way of generally understanding the material behaviour and the impact on magnetic and mechanical properties. So far, only bipolar bonded plate-like magnets are analysed in terms of the magnetic properties, which revealed no complex geometry or magnetic field structure.

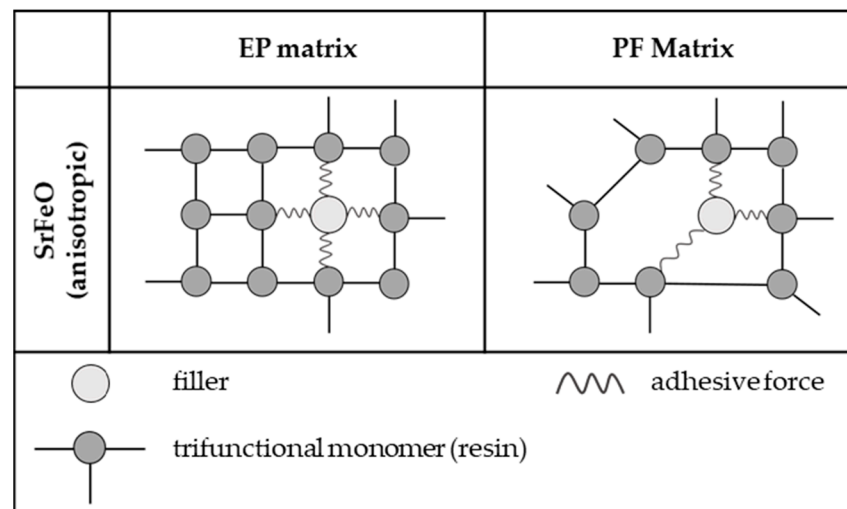


**Figure 1.** Integration of SrFeO in an EP and PF resin with respect to network theory; [in parts: [18]].

### 1.2. Fundamentals of Thermosets

Thermosets are based on oligomers which build an irreversible tri-dimensional network during the curing process by covalent bonds. This network has an amorphous structure and a higher cross-linking density compared to thermoplastics or elastomers [19]. The curing is initiated by temperature, pressure or chemical substances and generates at least two bonds between the oligomers. However, it is more likely that a high number of these bonds are built between single oligomers, which leads to the limitation that thermosets are not meltable and insoluble. This results in the general characteristic behaviour of a high temperature and media resistance, high surface hardness and mechanical behaviour with a brittle fracture [20]. Resins are subdivided into reaction and condensation resins. In reaction resins, a polyaddition or polymerisation takes place leading to a curing without a secondary product. Epoxy resin (EP) is a typical representative of reaction resins based on polyaddition [21]. Phenolic resin, which represents polycondensation resins for example, builds a secondary product during the curing. This product is likely to oxidize by coming in contact with metallic fillers [20].

The polyaddition and the polycondensation are subgroups of the step-group reactions. Within this reaction, two molecules with tri- or more functional groups in terms of thermosets build a new molecule with or without building a secondary product. Therefore, the chains of the oligomers are short for a longer period. In comparison, within the chain reaction, monomers are aligned and a chain is growing constantly [20]. These two reaction mechanisms lead to different polymerisation grades and reaction turnover. Within step growth reactions, the polymerisation grade is low for at least 50% of the turnover of the monomers, which results in a shift of the reaction turnover to longer times [22]. Particularly in thermoset systems, where fillers should be integrated or even orientated in terms of anisotropic fillers, a less sensitive behaviour towards the time is desirable.

### 1.3. Magnetic Properties

The magnetic properties can be described by the magnetic moment of a single electron and its rotation around its axis, and can therefore rely on the smallest magnetic unit [1]. In so-called ferromagnetic materials, all magnetic moments are oriented parallel and reach the highest total magnetic moment. Hard magnets, a subgroup of ferromagnetic materials, are also called permanent magnets as they have a characteristically high resistance against demagnetisation [23]. The hard magnetic fillers can be divided in two main groups: the rare earths and the ferrites. SrFeO, as a main representative of ferrites, exhibits a hexagonal geometry and is built by a reaction between Sr<sub>2</sub>O and Fe<sub>3</sub>O. In general, the particle size reaches rather low values between 1 and 10 µm; however, the particle size can be defined throughout the grinding process. The coercivity reaches up to 250 kA·m<sup>-1</sup> and the curie

temperature is 450 °C. NdFeB, is a rare earth or more precisely Nd<sub>2</sub>Fe<sub>14</sub>B, and as the customary type depicts a plate-like particle structure and a tetragonal crystal lattice with a general particle size of 100–400 µm. Again, the production process and the synthesis route influence the particle size. The coercivity of Nd<sub>2</sub>Fe<sub>14</sub>B reaches values between 870 and 2750 kA·m<sup>-1</sup> and is therefore much higher than SrFeO. However, the curie temperature reaches only 350 °C, which reveals about 100 °C lower value compared to SrFeO. Beside these differences, NdFeB has a two to three times larger resistance against demagnetisation compared to SrFeO [24].

Beside the two groups of hard magnetic fillers, the general behaviour of the particles can be divided into isotropic or anisotropic magnetic properties. The magnetic moments in isotropic fillers have a random orientation without a preferential direction. In terms of anisotropic fillers, the preferred orientation leads to a value of the remanence B<sub>R</sub>, which reaches about 85% of the saturation flux density B<sub>S</sub> relative to the filler content and the quality of the production process. In systems with isotropic fillers, B<sub>R</sub> obtains only 50% of B<sub>S</sub> [2]. The usage of higher magnetic properties in terms of anisotropic fillers leads to demand, and these fillers have to be oriented within the process. This can be realised by implementing a permanent magnet or an electromagnetic coil and a current through this conductor in the process. A further magnetisation of hard magnetic fillers can be realised within production or afterwards, for example, by an impulse magnetisation [25].

#### 1.4. Aim of the Paper

This paper aims to investigate the influence of matrix material and filler grade on the magnetic properties and filler orientations within multipolar-bonded magnets. Based on the general understanding of the impact of the material system on the flow and curing behaviour as well as the integration of fillers in the tri-dimensional network according to the network theory [17,18], the possibility of improving orientation within thermoset-based systems are discussed. More specifically, the impact of an epoxy resin (EP) and a phenolic resin (PF) on the hard magnetic filler SrFeO and a changing filler grade between 40 and 60 vol.-% on the filler orientation and corresponding magnetic properties are analysed. Further, the change in the properties along the sample depth is investigated with respect to the impact of the outer magnetic field strength. This behaviour is correlated with the network theory according to [18] and a general material characterisation. The investigations within this paper reveal important indications for the construction of thermoset-based bonded magnets, which should be fabricated in the injection-moulding process.

## 2. Materials and Methods

### 2.1. Materials

The matrix materials within these experiments were an epoxy resin (EP) called Epoxidur 368/1 and a phenolic resin (PF) called Resinol EPF 87120, both fabricated by Raschig GmbH (Ludwigshafen, Germany). The thermosets are a premixed powder with resin, hardener, catalyst and, in terms of EP, some carbon black pigments. However, the exact composition of the mixture is confidential and a business secret of Raschig GmbH. The important properties of the two materials are listed in Table 1, where the density  $\delta$ , the heat capacity  $c$  and the peak temperature  $T_{\text{peak}}$  are based on our own measurements, whereas the thermal conductivity  $\lambda$  relies on the manufacturer specification. The peak temperature  $T_{\text{peak}}$  was defined by a differential scanning calorimetry (DSC) according to DIN EN ISO 11357 with a constant rate of 10 K per minute in terms of EP and 5 K per minute in terms of PF in the first heating cycle between the temperature range of 0 °C and 300 °C. The difference in the heating rate is based on the variation of the chemical behaviour within the two types of thermosets.

**Table 1.** Specification of the matrix material in terms of the density  $\delta$ , heat capacity  $c$ , peak temperature  $T_{\text{peak}}$  (own measurements) and thermal conductivity  $\lambda$  (manufacturer specification).

Matrix Material	Density $\delta$ in $\text{g}\cdot\text{cm}^{-3}$	Heat Capacity $c$ in $\text{J}\cdot\text{g}^{-1}\cdot\text{C}^{-1}$	Thermal Conductivity $\lambda$ in $\text{W}\cdot\text{m}^{-1}\cdot\text{K}^{-1}$	Peak Temperature $T_{\text{peak}}$ in $^{\circ}\text{C}$
epoxy resin (EP)	1.225	1.616	0.4–0.6	170.1 <sup>(1)</sup>
phenolic resin (PF)	1.292	1.294	0.4–0.6	138.1 <sup>(2)</sup>

DSC: <sup>(1)</sup>: 10  $\text{K}\cdot\text{min}^{-1}$ ; <sup>(2)</sup>: 5  $\text{K}\cdot\text{min}^{-1}$ .

The experiments were based on the anisotropic hard magnetic filler strontium-ferrite-oxide (SrFeO) called OP-71 (Dowa Holdings Co., Ltd., Tokyo, Japan) and a varying filler grade of 40, 50, 55 and 60 vol.-%. Based on our own measurements, Table 2 reveals the main properties of the filler.

**Table 2.** Specification of the hard magnetic filler in terms of the density  $\delta$ , heat capacity  $c$ , thermal conductivity  $\lambda$  and mean particle size  $d_{50}$  (own measurements).

Hard Magnetic Filler	Density $\delta$ in $\text{g}\cdot\text{cm}^{-3}$	Heat Capacity $c$ in $\text{J}\cdot\text{g}^{-1}\cdot\text{C}^{-1}$	Thermal Conductivity $\lambda$ in $\text{W}\cdot\text{m}^{-1}\cdot\text{K}^{-1}$	Mean Particle Size $d_{50}$ in $\mu\text{m}$	
				Numerical	Volumetric
strontium-ferrite-oxide (SrFeO)	5.380	0.639	2.3	4.87	1.94

The density was analysed using a gas pycnometer (type: AccuPyc 1330; Micromeritics GmbH, Unterschleißheim, Germany). The specific heat capacity  $c$  was determined for 25  $^{\circ}\text{C}$  using the C80 calorimeter (type: 3D-Calvet calorimeter; TA Instruments, New Castle, DE, USA). Further, the thermal conductivity  $\lambda$  of the filler material was determined at 23  $^{\circ}\text{C}$  by using an extrapolation based on the Lewis–Nielsen equation of measurements of the thermal conductivity  $\lambda$  based on compounds, where plate-like samples were analysed in a HotDisk (C3 Prozess- und Analysetechnik GmbH, Haar, Germany). The mean particle size was evaluated using an optical camera with static image analysis (Morphology G3s, Malvern Panalytical GmbH, Kassel, Germany). The volume of the measured filler samples was 5  $\text{mm}^3$ , counting up to 80,000 particles in one measurement.

## 2.2. Fabrication of the Test Specimens

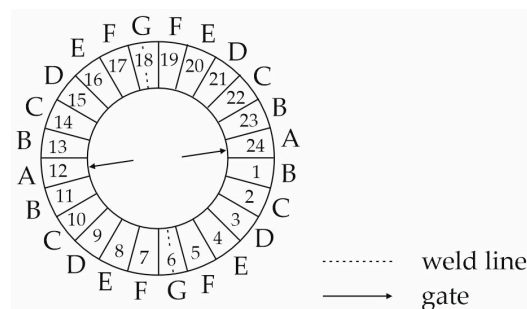
The first step of the fabrication of the test specimens was the production of the compound using a twin-screw extruder (type: KrausMaffei Berstorff ZSE 25Ax45D, KrausMaffei Group, Munich, Germany) with a constant speed of 80  $\text{min}^{-1}$ . The two components of the material were manually premixed with the definition of the proportion by using a high-precision weighted device before the placing in the extruder. The temperature was set between 50  $^{\circ}\text{C}$  at the entry and 90  $^{\circ}\text{C}$  at the nozzle, so that a curing of the material within the extruder was rejected. The cooling was realised by a vibratory feeder, followed by a pelletising.

The second step of the fabrication was the injection moulding of the multipolar ring samples. Therefore, an injection-moulding machine (type: KrausMaffei KM 80-380 CX DUR/03, KrausMaffei Group, Munich, Germany) with a screw diameter of 30 mm was used. The different process parameters relative to the matrix type are shown in Table 3. As the two resin types differ in reaction kinetics, curing mechanism and general viscosity behaviour, the process conditions had to be adopted to each of the two types. The long gelation time of EP is far from an economical standard. Further optimisation of the compound has to be done regarding this point.

**Table 3.** Process parameters of the fabrication of multipolar ring samples with differentiation between the two resin types of EP and PF.

Process Conditions	EP	PF
mass temperature $T_m$ in °C	85	85
mold temperature $T_{WZ}$ in °C	190	180
holding pressure $p_h$ in bar	650	650
heating time $t_h$ in s	200	45
injection speed $v_{in}$ in $\text{mm}\cdot\text{s}^{-1}$	15	15

The multipolar bonded ring had an outer diameter of 50.6 mm, an inner diameter of 22.6 mm and a width of 5 mm. The gating system was a two pinpoint system placed on the inner diameter at the middle of the pole. The material of the sleeve, which separated the outer permanent magnets and the cavity, was ferro-titanite-cromoni with a low magnetic permeability. The samples revealed 24 poles equally distributed on the circumference. These poles can be summarised into seven characteristic poles named from A to G, as shown in Figure 2. Here, the pole at the gating position has the numbers 12 and 24, but is classified by A as representative of the gate. Similarly, pole G represents the weld line at the pole numbers 6 and 18.

**Figure 2.** Multipolar-bonded ring sample with 24 poles and representative seven characteristic poles (A to G) relative to the position on the circumference.

### 2.3. Characterisation

#### 2.3.1. Differential Scanning Calorimetry (DSC) According to DIN EN ISO 11357 [26]

To define the temperature and time dependent reaction kinetic of the compound, a differential scanning calorimetry (type: DSC 2500, TA Instruments, New Castle, DE, USA) was used. Within this measurement, about 5 mg of the sample was placed into an aluminium pane and, in term of the dynamic measurements, the two heating cycles were conducted with different heating rates relative to the sensitivity of the material regarding temperature. Accordingly, a rate of 10 K per minute in terms of EP and 5 K per minute in terms of PF was chosen. The measurements were held between 0 °C and 300 °C for both cycles under a nitrogen atmosphere. The classification of the dynamic reaction kinetics was based on the specific enthalpy  $\Delta H_{ges;1}$ , the peak temperature  $T_{Peak}$  and the reaction turnover  $\alpha$  (according to Equation (1)) in the first heating cycle as well as the degree of curing  $\Sigma_{curing}$  (according to Equation (2)) in the second heating cycle with respect to Equations (1) and (2).

$$\alpha = \frac{\Delta H_j}{\Delta H_{ges;1}} \quad (1)$$

$$\Sigma_{curing} = \left(1 - \frac{\Delta H_{ges;1}}{\Delta H_{ges;2}}\right) \cdot 100\% \quad (2)$$

Further, the time-dependent reaction kinetics were defined using an isothermal DSC measurement set up with a temperature level of 100, 110 and 120 °C for EP and 122, 124, 126 °C for PF. The classification of the static reaction kinetics was based on the specific enthalpy  $\Delta H_{ges;1}$  and the peak time  $t_{Peak}$ .

The general route of the DSC measurement of a dynamic measurement is the route with one maximum. The temperature, where this maximum is reached, depicts the peak temperature  $T_{\text{Peak}}$  and the specific enthalpy  $\Delta H_{\text{ges};1}$  correlated with the area underneath the maximum. Within the isothermal DSC, the route reveals a fast increase and maximum at the beginning. Depending on the temperature level, the time span until a constant value after the maximum is reached changes.

### 2.3.2. Determination of the Viscosity Behaviour Based on a Rotational Viscometer According to DIN EN 53019 [27]

The viscosity behaviour was defined using a rotational viscometer (type: Discovery Hybrid Rheometer 2, TA Instruments, New Castle, DE, USA) based on two plates with a shearing load. After reaching the starting set up of each measurement, a shell was placed around the sample to ensure that the chamber was floated with nitrogen. The temperature dependence of the viscosity was conducted in terms of dynamic measurements and the time dependence in terms of isothermal measurements. In the case of the dynamic behaviour, the samples were analysed between 80 °C and 200 °C with a heating rate of 5 K per minute. The viscosity behaviour was characterised in terms of the minimum viscosity  $\eta_{\text{min}}$ . The isothermal measurements started at a defined temperature, which was held constant during each set up, and the change of the viscosity relative to the time was defined. The level of the temperature was set between 120 °C and 160 °C in 10 °C steps. As the route of  $\eta$  follows an s slope, the time  $t_{\text{tp}}$  between the beginning of the measurement and the turning point was analysed.

### 2.3.3. Magnetic Properties before and after Full Magnetisation

To define the full magnetic potential of the samples and to differentiate between the orientation and partial magnetisation within the cavity as well as the full magnetisation after the fabrication of the sample, the magnetic properties were defined in two steps. Within the first step, the magnetic properties after the production of the samples were analysed using a test rig, as shown in Figure 3. These properties were based on a possible orientation of the fillers, a partial magnetisation during the fabrication process and the integrated outer magnetic field. The samples were placed in a defined position using a clamping device and the route of the magnetic flux density relative to the circumference was recorded by a hall sensor (Magnet-Physik Dr. Steingroever GmbH, Cologne, Germany) and a rotary encoder (Heidenhain GmbH, Traunreut, Germany). The sample was placed on a shaft, which was driven by a motor with a constant speed.

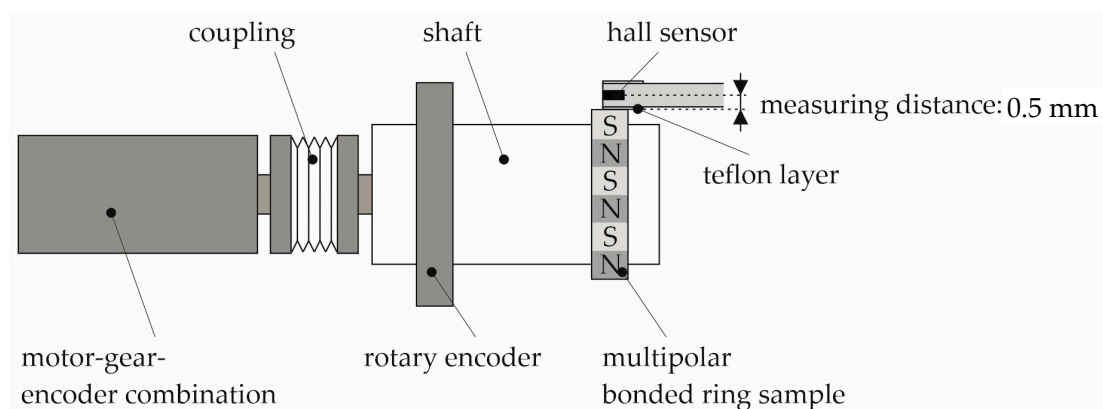


**Figure 3.** Test rig for evaluating the multipolar bonded ring samples based on the magnetic flux density on the circumference.

The magnetic properties based on the magnetic flux density relative to the circumference were defined by the maximum of the peak flux density  $|B_{R,\text{max}}|$  at the seven characteristic poles relative to Figure 2. To compare these values with the magnetic properties after full magnetisation, samples with the dimension of  $5 \times 5 \times 5 \text{ [cm}^3\text{]}$  were prepared out of the

characteristic poles A, D and G with a milling machine. The final magnetisation was ensured using a pulse magnetizer (type: Im-12220-U-MA-C, Magnet-Physik Dr. Steingroever GmbH, Cologne, Germany) and a magnetic device (type: MV D30 × 30 mm F-TC, Magnet-Physik Dr. Steingroever GmbH, Cologne, Germany). Afterwards, the remanence  $B_R$  was defined by a permagraph (type: C-300, Magnet-Physik Dr. Steingroever GmbH, Cologne, Germany).

Further, the change of the magnetic properties along the sample depth was defined on the characteristic pole D, exemplary, to compare the results of the orientation of the fillers with the magnetic properties. Therefore, the characteristic pole D was prepared out of the sample along the full depth using a milling machine. After a final magnetisation step, the remanence  $B_R$  was defined on the inner diameter using a hall sensor (Magnet-Physik Dr. Steingroever GmbH, Cologne, Germany). After that, a defined height of 2 mm was removed by a grinding machine and the remanence  $B_R$  was again calculated on the inner diameter. These two steps were repeated until the outer diameter was reached by a distance of 2 mm. In total, seven measuring steps were evaluated.

#### 2.3.4. Determination of the Orientation of the Fillers

The orientation of the fillers was defined in the middle of the sample width using prepared samples out of the multipolar bonded ring. This preparation was realised by a water-cooled saw with minimal temperature input in the region of the characteristic pole A (near the gate), C and D (in the middle between gate and weld line) as well as G (near the weld line). The prepared samples were embedded in cold-curing epoxy resin (type: Epofix, Struers GmbH, Ottenssoos, Germany) and polished afterwards. The images were taken using a stereo microscope (type: Axio Zoom.V16, Carl Zeiss AG, Oberkochen, Germany) differing between the position relative to the characteristic poles and the sample depth. The images, taken at the pole pitch, were defined by I to III, at the middle of the pole by i to ii and along the depth by 1 to 5. Figure 4 depicts the sample preparation (A) as well as the different positions for the orientation analysis (B–E).

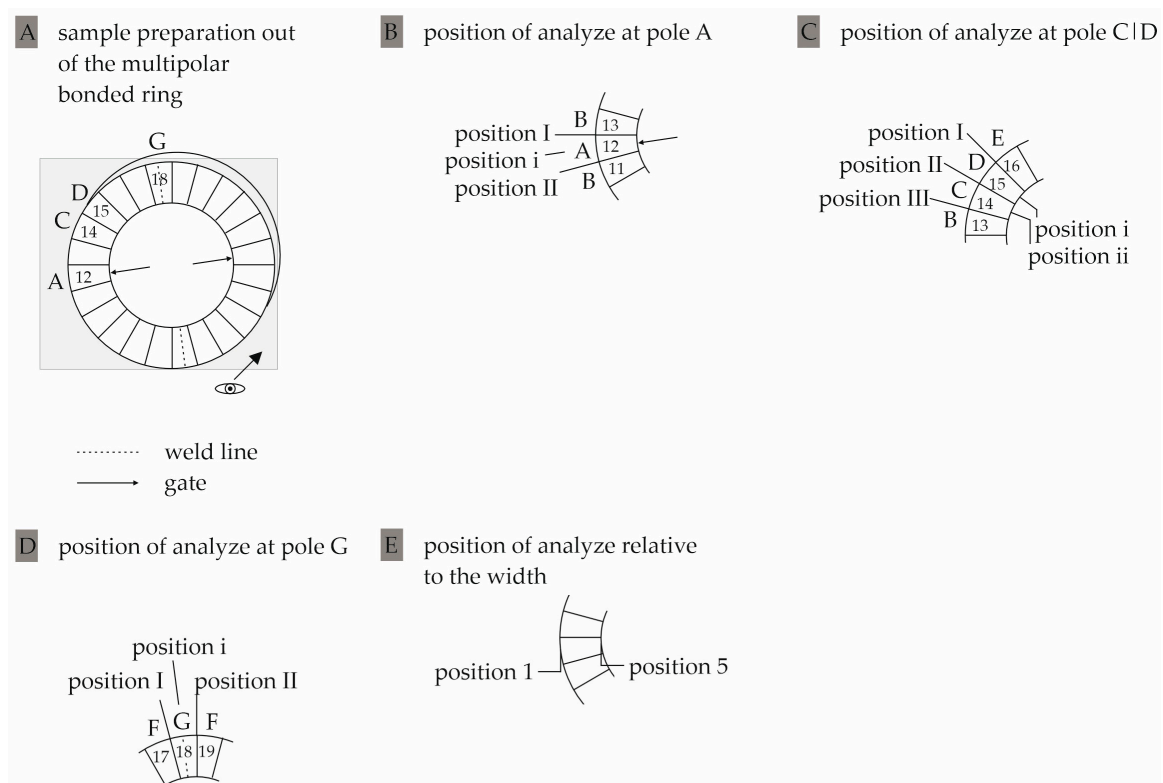


**Figure 4.** Preparation of the samples for characterising the orientation of the fillers based in multipolar rings (A), position of analyses relative to the pole (B–D) and to the depth (E).

Using a grey scale threshold analysis, the matrix material and the fillers could be separated within the images. The longest axis of each filler was defined automatically and the orientation between  $0^\circ$  and  $90^\circ$  was analysed with respect to this axis of each particle.

### 3. Results

#### 3.1. Reaction Kinetics Based on Differential Scanning Calorimetry (DSC)

The change of the specific heat enthalpy  $\Delta H_{\text{ges};1}$  and the peak temperature  $T_{\text{Peak}}$  relative to the filler grade and the matrix material in the thermoset-based compound with the filler SrFeO is shown in Figure 5. With respect to  $\Delta H_{\text{ges};1}$  of the pure matrix material, the value of  $\Delta H_{\text{ges};1}$  is significantly reduced in the filled systems. Further reduction takes place in the increase of the filler grade between 40 and 60 vol.-%. This reduction is more present in the matrix material EP, as  $\Delta H_{\text{ges};1}$  within PF is already reduced with a filler grade of 40 vol.-%. Increase of the filler grade has only a small impact on  $\Delta H_{\text{ges};1}$ . With a filler grade of 60 vol.-%, the difference in the value of  $\Delta H_{\text{ges};1}$  between the two matrix materials is almost gone, likely because of the large amount of fillers not involved in the curing process. In general, PF-based systems reveal a smaller amount of  $\Delta H_{\text{ges};1}$  during the reaction and a lower value of  $T_{\text{Peak}}$ .  $T_{\text{Peak}}$  is hardly affected by the different filler grades and reveals only a change due to the matrix material.

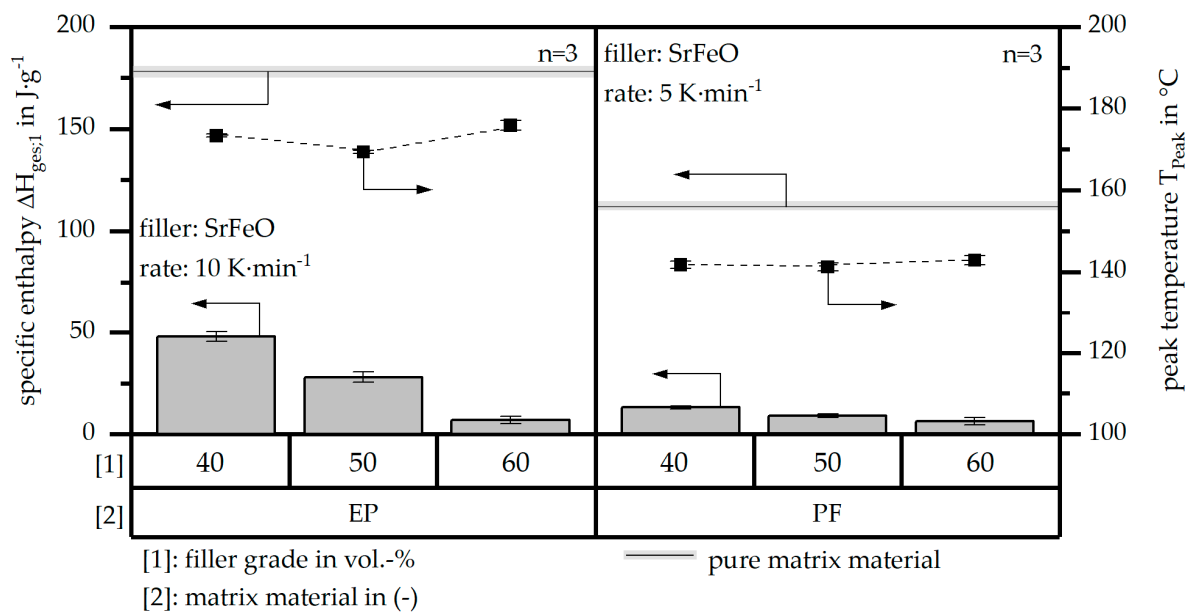


**Figure 5.** Impact of the filler grade and the matrix material onto the specific heat enthalpy  $\Delta H_{\text{ges};1}$  and the peak temperature  $T_{\text{Peak}}$  in the first heating cycle.

Figure 6 depicts the influence of the two matrix materials on the degree of curing  $\Sigma_{\text{curing}}$  (A) and the reaction turnover  $\alpha$  (B), whereby the influence of the different filler grades is only shown in terms of  $\Sigma_{\text{curing}}$ . The filler grade has only a little impact on  $\alpha$  with the tendency to shift the route of  $\alpha$  towards lower temperatures with increasing filler grades.  $\Sigma_{\text{curing}}$  is reduced with increasing filler grades but reaches a higher value in terms of EP compared to PF as a matrix material. As EP reveals a high integration of the filler into the network structure, as shown in [18], the impact of the increasing filler grade onto the reduction of  $\Sigma_{\text{curing}}$  is greater compared to an PF matrix, but on a higher level. In an EP matrix, the fillers hinder the further curing to some extent, as the fillers reveal adhesive forces to the tri-dimensional monomers and link the network structure. PF based systems produce a secondary product in the curing process, leading to a further reduction of  $\Sigma_{\text{curing}}$  compared to EP. However, integration of the filler is less in a PF-based matrix, which reduces the impact of the changing in the filler grade. As shown in Figure 6B, the reaction turnover  $\alpha$  is shifted to higher temperatures in the filled systems compared to the unfilled

ones. PF-based systems reveal a shift to lower temperatures relative to EP-based systems, as it was already depicted in terms of the different values of  $T_{Peak}$ . After  $T_{Peak}$  of PF is about 30 °C lower compared to EP, the main impact of the enthalpy change happens at a lower temperature compared to EP. The reaction turnover  $\alpha$  shows the range of the change of the enthalpy based on DSC measurements and has its turning point at the temperature, where the dynamic DSC measurement reaches its maximum. Therefore, a lower  $T_{Peak}$  indicates a shift in the reaction turnover  $\alpha$  of PF relative to EP. It can be assumed that the difference in the reaction of EP and PF and the building of secondary products throughout the chemical reaction might be one factor hindering the reaction at higher temperatures. With respect to Tables 1 and 2, the heat capacity  $c$  is reduced in terms of the filler and the thermal conductivity  $\lambda$  is increased. It is assumed that the reduction of  $c$  has a greater impact on the curing process and is mainly responsible for  $\alpha$  shifting to higher values in the filled system.

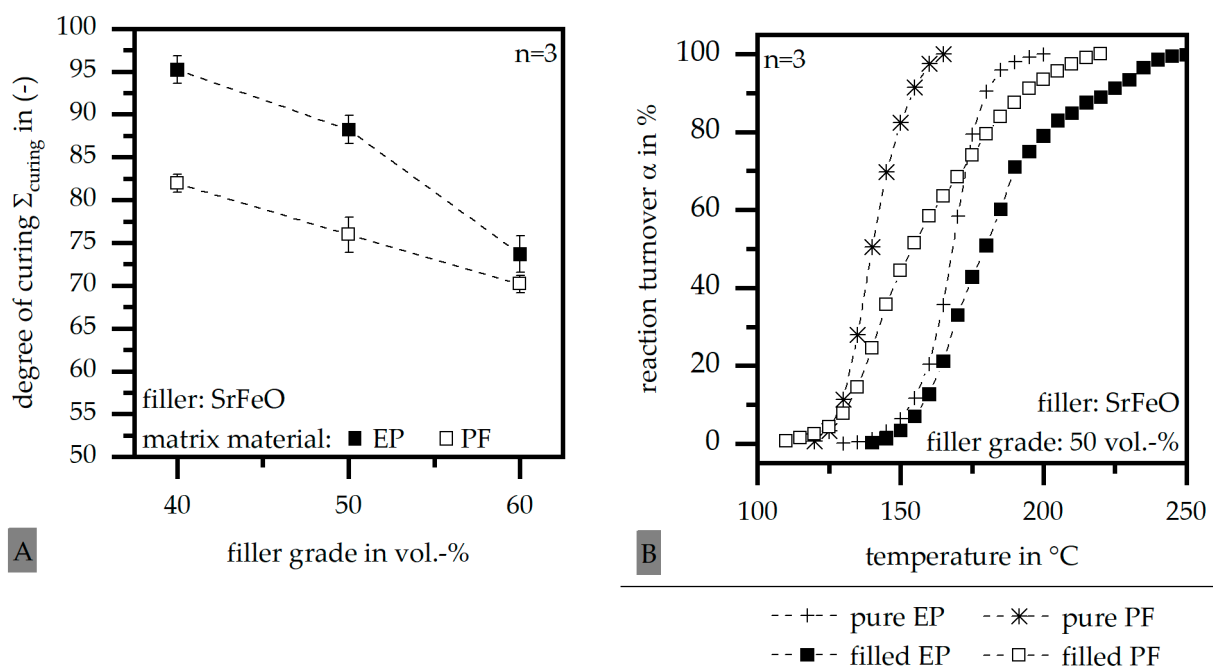


**Figure 6.** Impact of the filler grade and the matrix material on the degree of curing  $\Sigma_{curing}$  (A) as well as the impact of the matrix material on the reaction turnover  $\alpha$  compared to the pure matrix material (B).

The impact of the matrix material on the specific heat enthalpy  $\Delta H_{ges;1}$  and the peak time  $t_{Peak}$  of the isothermal measurements and a constant filler grade of 50 vol.-% is shown in Figure 7. PF reveals only a small range of the temperature levels where the isothermal DSC can be conducted.  $\Delta H_{ges;1}$  is hardly affected by the different matrix systems, with a small increase of  $\Delta H_{ges;1}$  with higher isothermal temperature levels. An exact trend of the change of  $\Delta H_{ges;1}$  relative to the isothermal temperature level cannot be seen due to high values of standard deviation. The peak time  $t_{Peak}$  is significantly reduced in terms of an EP-based system, with higher isothermal temperature levels. This effect can hardly be seen in PF, likely because of the small range of temperature levels. Nevertheless, an increasing value of the temperature level within the curing process reduces the peak time  $t_{Peak}$  significantly, with PF revealing a slightly lower time gap relative to EP, and increases  $\Delta H_{ges;1}$  independent to the matrix material to some extent.

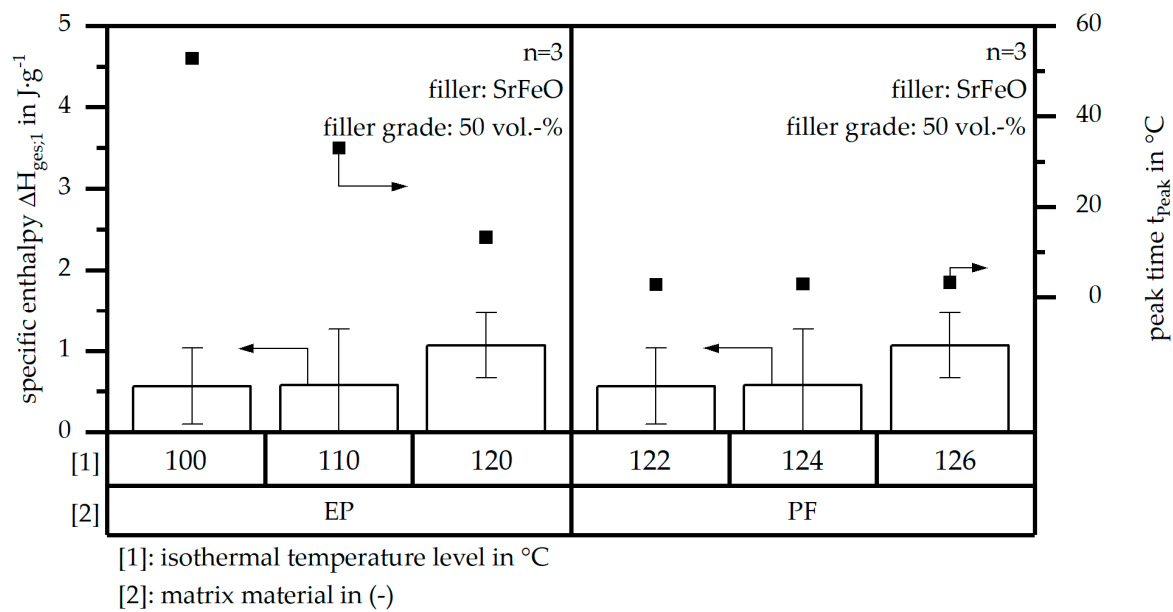


**Figure 7.** Impact of the matrix material onto the specific heat enthalpy  $\Delta H_{ges,1}$  and the peak time  $t_{peak}$  with respect to different isothermal temperature levels.

### 3.2. Viscosity Behaviour Based on Rotational Viscometer

The minimum of viscosity  $\eta_{min}$  relative to the filler grade and the matrix material is depicted in Figure 8A. Further, the change of the pot life  $t_{tp}$  with respect to the matrix material is shown in Figure 8B with a constant filler grade of 55 vol.-%. With increasing filler grade,  $\eta_{min}$  rises as well, showing almost a linear relationship between the increase of the filler grade and  $\eta_{min}$  despite the logarithmic scale. PF reveals slightly higher values in terms of  $\eta_{min}$  compared to EP. However, both materials show significantly higher values for  $\eta_{min}$  compared to the pure matrix material, with an increase of the minimum of the viscosity by at least three decades in terms of a filler grade of 40 vol.-% and four decades by 60 vol.-%. This goes along with the network structure, as shown in [18], where the increasing filler grade results in a higher number of linked junctions in the network, which decreases the flow ability tremendously. In general,  $t_{tp}$  is reduced with an increasing isothermal temperature level in the range from 120 °C to 160 °C. The values of  $t_{tp}$  are lower in terms of filled system, but the difference between the material systems is reduced in PF compared to EP and significantly with the increasing isothermal temperature level.

### 3.3. Magnetic Properties before and after Full Magnetisation

The magnetic properties displayed are the maximum of the peak flux density  $|B_{R,max}|$  before the final magnetisation step and in the remanence  $B_R$  after the magnetisation. Figure 9 depicts the influence of the matrix material, a constant filler grade of 55 vol.-% (A), and the impact of the filler grade, the matrix material PF (B), on both parameters of the magnetic properties. The influence of the second magnetisation step is significant independent to the material system and is based on the reduced outer magnetic field strength due to the high tool temperature. Therefore, thermoset-based polymer bonded magnets need a further magnetisation after the fabrication to ensure the use of the magnetic potential. The remanence  $B_R$  of PF based systems is slightly higher compared to EP-based compounds and reaches about 83% of the ideal magnetic properties. EP-based systems obtain 72% of the ideal value with respect to the filler type and grade. With respect to the reduction of the filler grade, the magnetic properties are lower and reach only 57% of the ideal value in terms of 40 vol.-% filler grade. Taking this into account, the high  $B_R$  of 55 vol.-% of a PF matrix is not only reached due to the matrix material but also affected by the amount of fillers and their interaction. It can be assumed that the matrix material defines the integration of the fillers in the network, according to [18], but further, the filler grade defines

the support between the fillers. Therefore, a certain amount of fillers is needed to improve the orientation between the fillers among each other to reach the full ideal value of the magnetic properties. However, if the filler grade is too high, interactions between the fillers become more likely, which again hinders the full orientation. Beside the influence of the matrix material and the filler grade, Figure 9 also shows the influence of the position of the pole on the magnetic properties. Within the characteristic pole G,  $B_R$  is reduced. This could be attributed to a lack within the orientation at the weld line, possibly due to porous flow front, which is likely in terms of a thermoset.

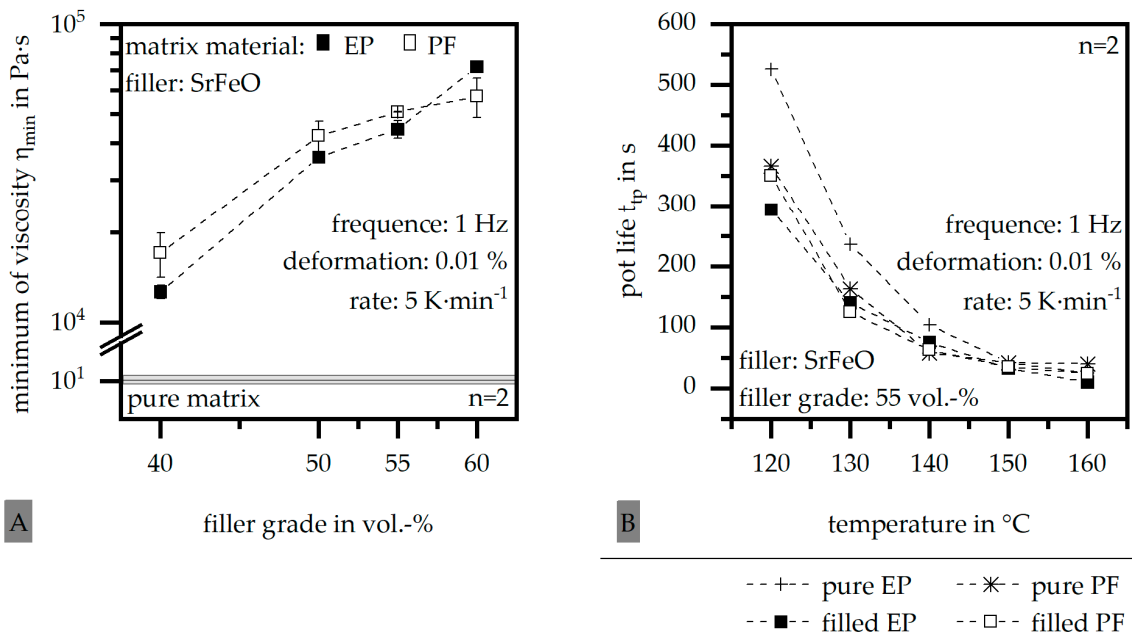


**Figure 8.** Impact of the filler grade and the matrix material onto the minimum of viscosity  $\eta_{\min}$  (A) and influence of the matrix material on the pot life  $t_{tp}$  (B) relative to pure matrix material.

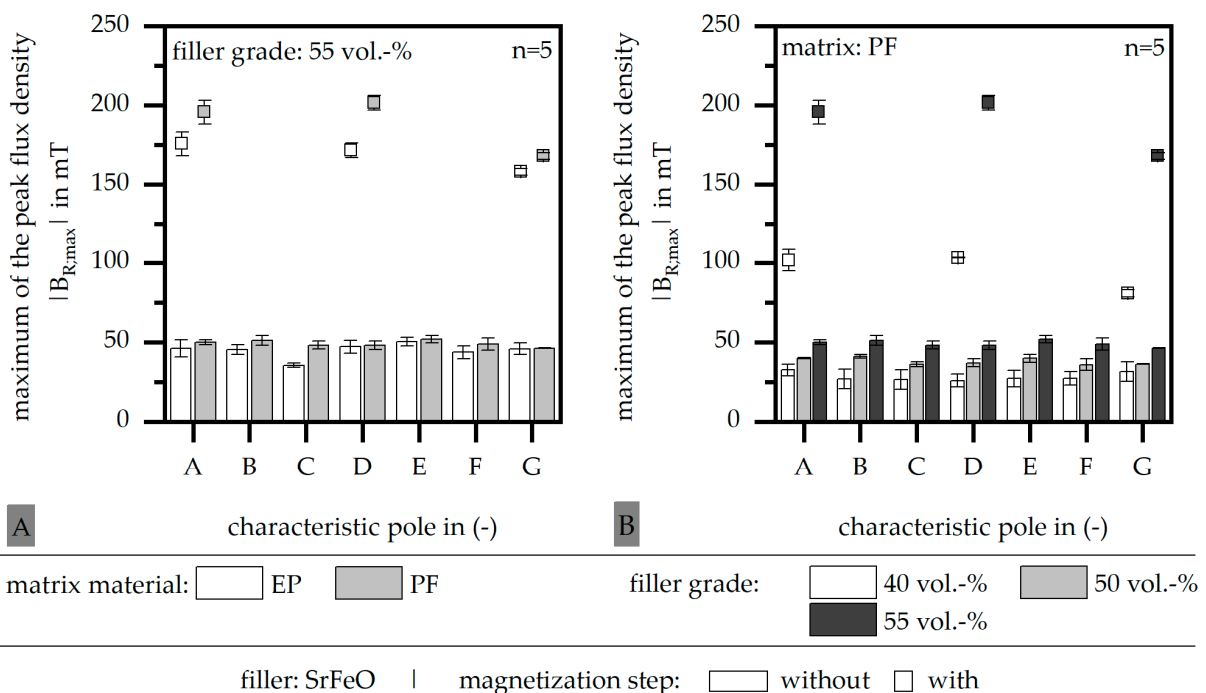


**Figure 9.** Impact of the matrix material (A) and the filler grade (B) on the magnetic properties before and after magnetisation.

The change of the magnetic properties along the sample depth is portrayed in Figure 10 with respect to the impact of the matrix material (A) and the filler grade (B). The remanence  $B_R$  increases along the changing positions, reaching a higher value as the position gets near the outer diameter. Despite the difference in the matrix material and the filler grade, a significant rise in  $B_R$  appears at 8 mm away from the outer diameter [measuring point 4]. After this measuring point, the increase of  $B_R$  is low and runs into a plateau. This reveals that the magnetic properties are similar within the range of about 8 mm from the outer diameter, which is likely to correlate with a proper orientation within this area. The change of the magnetic properties and the general route along the sample depth is quite similar within the two matrix materials, and changes with respect to the filler grade. If the filler grade is only 40 vol.-%, there is no significant increase of  $B_R$ , likely because the orientation takes place only in a small area near the outer diameter. As the filler grade is quite low, a supportive effect between the fillers is not likely; therefore, the weak outer magnetic field strength has a high impact, reaching less orientation and low magnetic properties compared to a higher filler grade of 55 vol.-%. This can also be seen in a comparison of the ideal magnetic properties and the filler grade, assuming a full orientation. The remanence  $B_R$  of the pure filler SrFeO is 439 mT according to our own measurements. If the filler grade reaches only 40 vol.-%, the remanence  $B_R$  is only 40% of the pure filler value and can reach maximal 175 mT. With a filler grade of 55 vol.-%, this maximum is at a value of 242 mT. Comparing these ideal values with the values reached according to Figure 10B, the sample with 40 vol.-% filler grade reaches only 57% of the ideal value at the outer diameter and 43% at the inner diameter. The sample with 55 vol.-% filler grade reaches 83% of the ideal value at the outer diameter and 52% at the inner diameter, which clearly depicts an improvement in the filler orientation with increasing filler grade. Due to the higher filler grade, the distance between the fillers decreases, which makes it more likely that fillers interfere with each other. This often leads to a so-called stack accumulation, where the orientated filler influences the next filler and orientates it as well. This can only take place if the distance between the fillers is low enough.

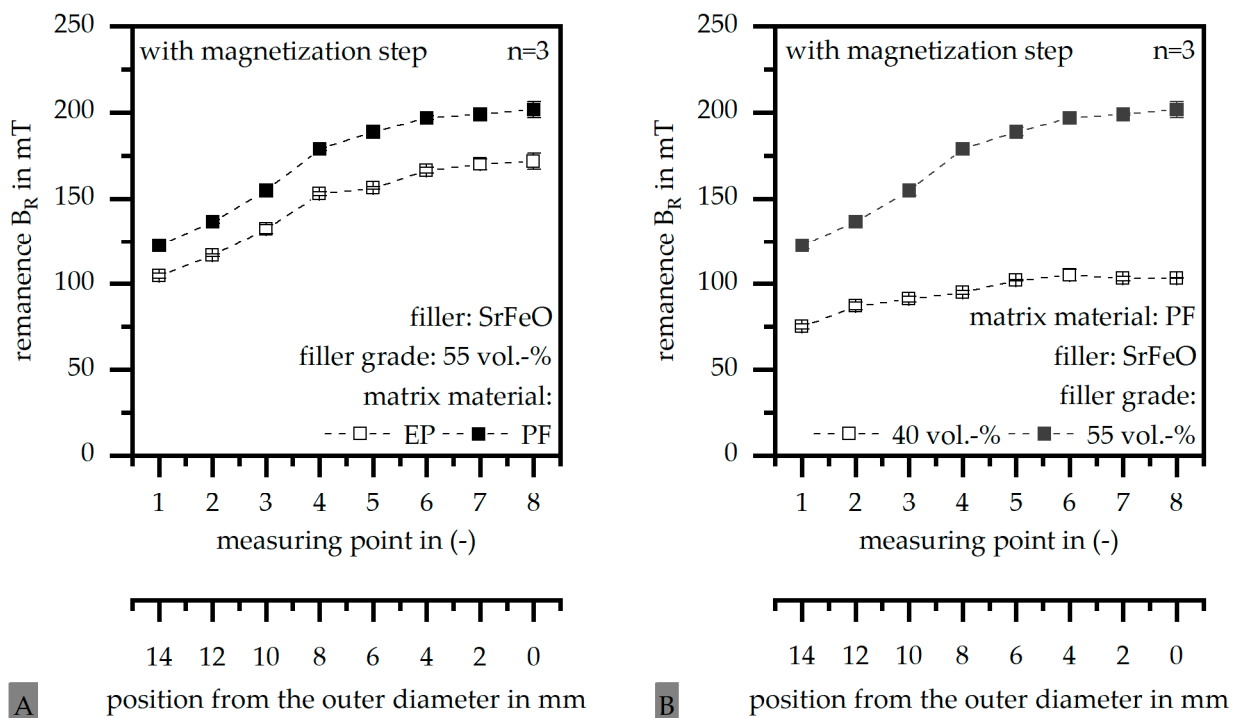


**Figure 10.** Impact of the matrix material (A) and the filler grade (B) on the magnetic properties along the sample depth.

### 3.4. Hard Magnetic Filler Orientation

The change of the orientation at the characteristic poles A, D and G at the pole pitch and in the middle of the pole on the outer diameter of the ring sample is depicted in Figure 11, in terms of the influence of the matrix material. The expected orientation in the middle of the pole is 0°, which is reached independent to the matrix material. However, the orientation in the middle of the pole is narrow for PF and broader for EP. In the pole pitch, the orientation should reach 90°. Both matrix materials reveal an orientation between 60° and 90° in the pole pitch, but again PF reaches a narrow distribution compared to EP. With that, the reduction of the magnetic properties of EP is at least partly based on less orientation. Further, Figure 11 depicts that within one sample, the orientation in one position is repeatable. This can be seen, for example, by comparing the pole pitch position I and II in the sample. The orientation at the characteristic poles reveals no significant difference between each other and therefore, does not suggest that it is reduced in the characteristic pole G. With that, the lower values of the magnetic properties in pole G cannot be described in terms of the orientation.

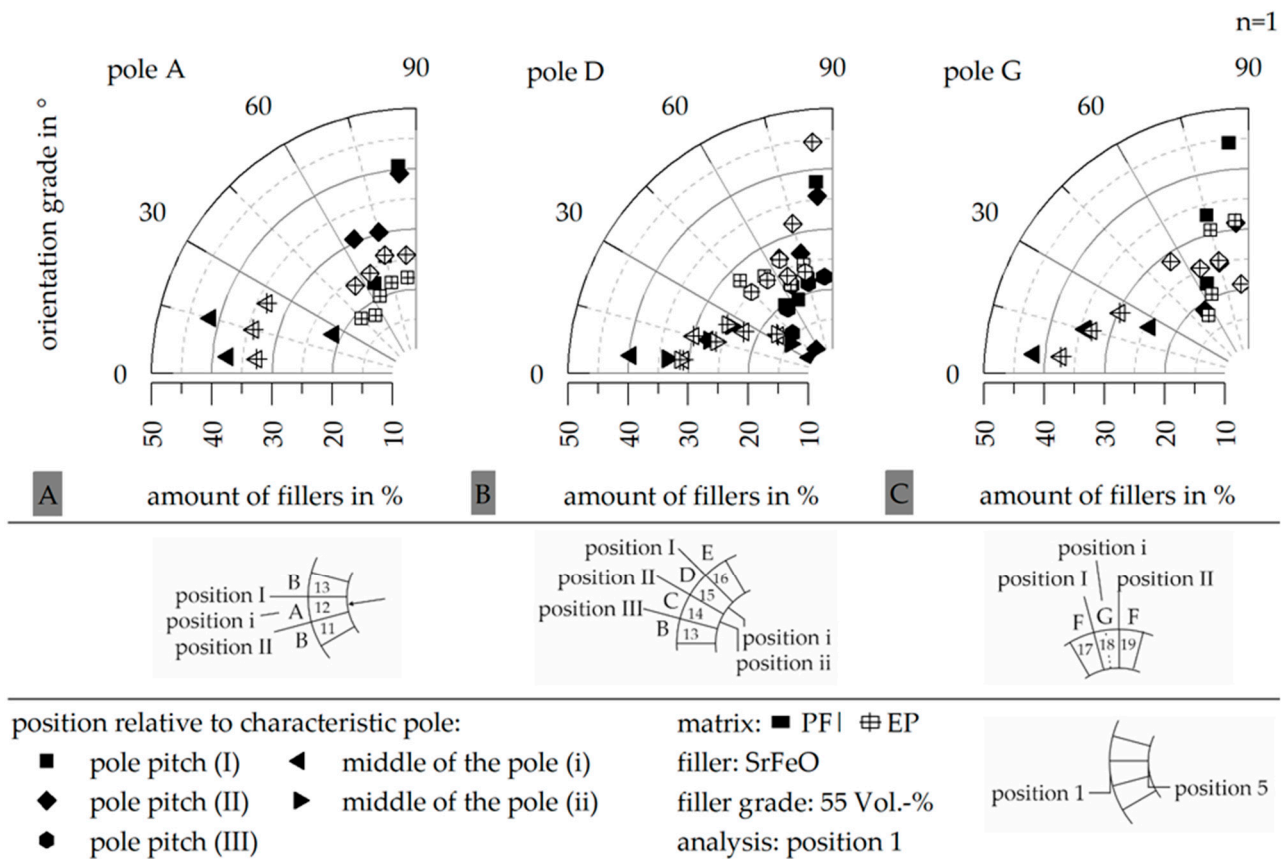


**Figure 11.** Impact of the matrix material on the orientation of the fillers at the characteristic pole A (A), pole D (B) and pole G (C) relative to pole pitch and middle of the pole on the outer diameter (position 1).

Besides the orientation on the outer diameter, the orientation along the sample depth has to be evaluated to define the possible orientation within the sample, with respect to the outer magnetic field strength. Figure 12 depicts the orientation along the sample depth of a PF-based material system for the characteristic poles A, D and G at the pole pitch (A–C) and in the middle of the pole (D–F). Especially for the characteristic pole D and G in the pole pitch, the orientation is reduced if the position is more than 7 mm away from the outer diameter. At these positions [position 4 and 5], the orientation in the pole pitch reaches no preferred orientation and depicts a range of orientation between 30° and

90°, with almost the same amount of fillers at each angle segment. A similar behaviour can be seen in the middle of the pole, where the orientation is significantly reduced at positions 4 and 5 without reaching a preferred orientation. Therefore, the outer magnetic field strength of the PF-based material systems and with respect to the tool temperature used in Table 3, is appropriated to orientate the hard magnetic filler SrFeO within a sample depth of 7 mm. Further increase of the sample depth would not improve the orientation if the outer magnetic field strength or the tool temperature were not adapted.

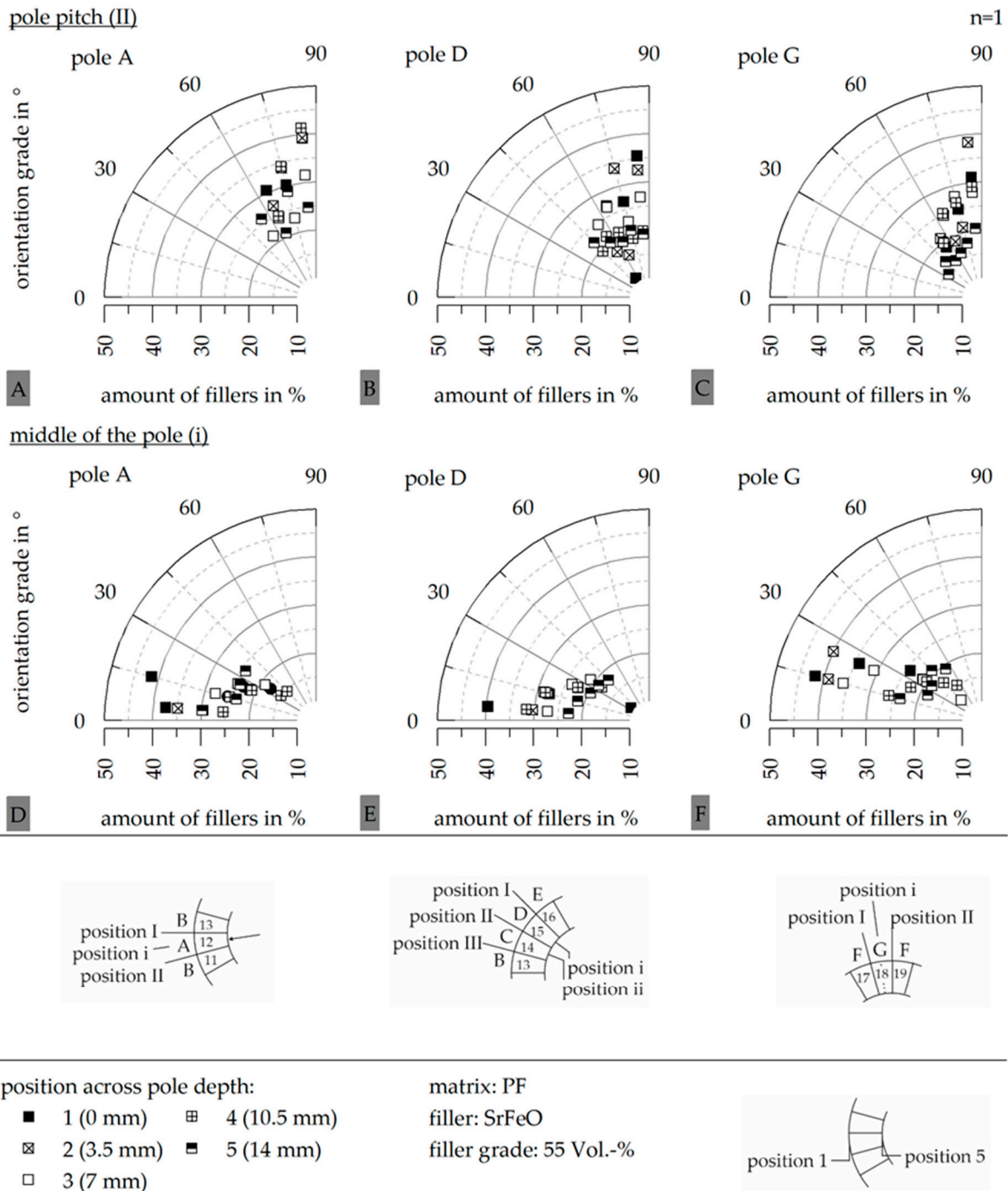


**Figure 12.** Orientation of the fillers at the characteristic pole A (A,D), pole D (B,E) and pole G (C,F) relative to pole pitch (II) and middle of the pole (i) across the pole depth for the matrix material PF.

Similar to the PF-based material system, Figure 13 depicts the orientation along the sample depth for EP-based compounds with respect to the pole pitch (A–C) and the middle of the pole (D–F) at the characteristic pole A, D and G. In the pole pitch, the border between a good and a weak orientation is sharper for EP than for PF. Again, an orientation within a sample deeper than 7 mm is not possible.

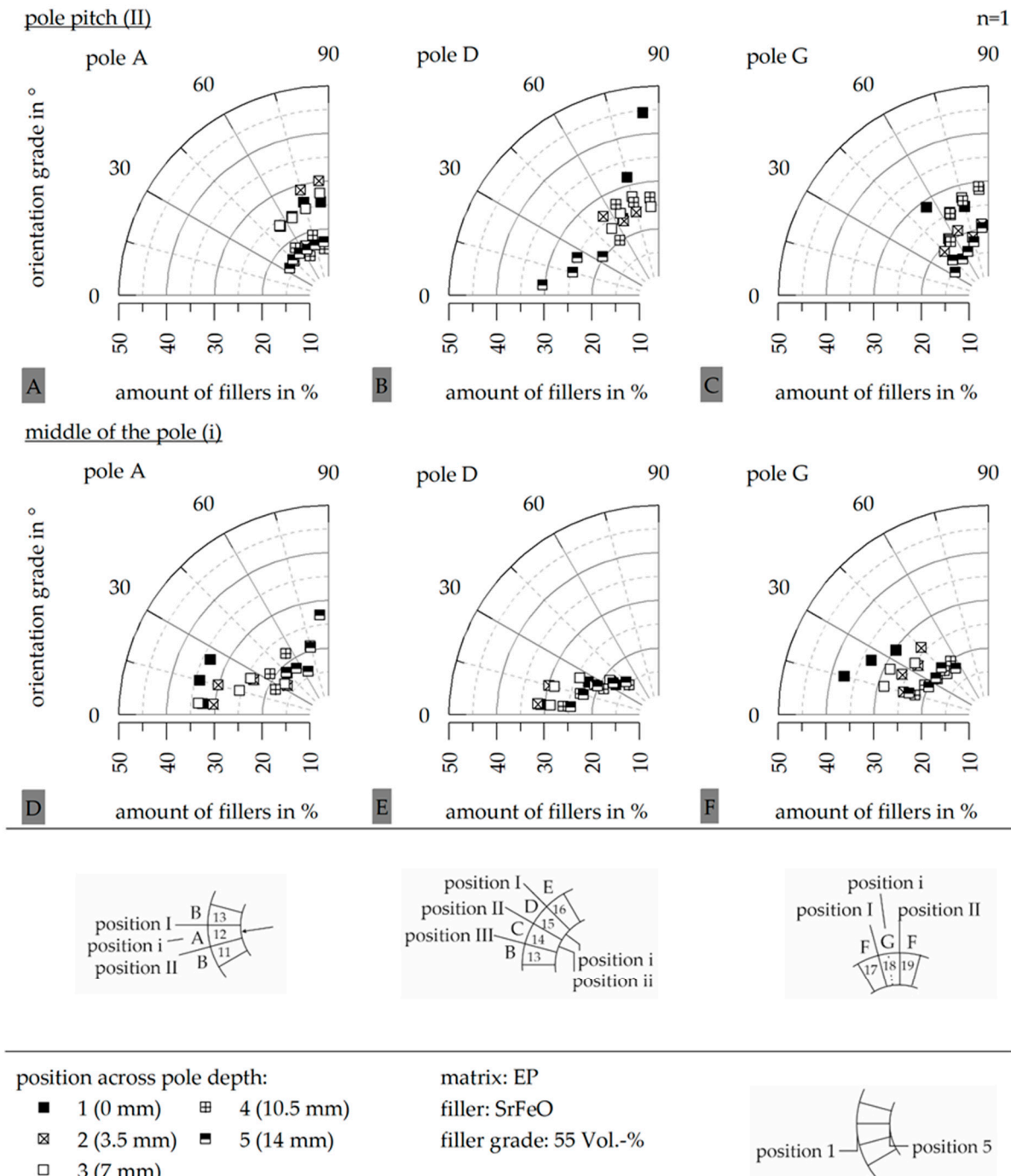


**Figure 13.** Orientation of the fillers at the characteristic pole A (A,D), pole D (B,E) and pole G (C,F) relative to pole pitch (II) and middle of the pole (i) across the pole depth for the matrix material EP.

#### 4. Discussion

The change of the magnetic properties of the matrix material and the filler grade in a multipolar bonded ring magnet is mainly based on the network structure and with that, the integration of the fillers in the tri-dimensional linked monomers of the thermoset matrix.

As depicted in [18], EP-based systems reveal a strong integration of the hard magnetic filler SrFeO, whereas PF-based systems show a weaker integration with only a few cross-linking positions. Further, the reaction mechanism between EP and PF is highly different, with PF building a secondary product in the curing process. This effects the degree of curing  $\Sigma_{\text{curing}}$ , for example, where PF reveals a lower level relative to EP, but has less impact on the changing filler grade. The different reaction mechanisms between EP and PF lead to a shift in the reaction of PF towards lower temperatures and less needed enthalpy. However, PF-based systems reach higher magnetic properties and an increase in the orientation at the pole pitch and the middle of the pole, mainly due to the possibility of higher mobility in the fillers within the network. Therefore, the partial integration of the fillers in a PF-based system, as shown in [18], leads to an improvement of the orientation and a narrow distribution of the preferred orientation. Further, a high filler grade of 60 vol.-% improves the orientation between the fillers and therefore increases the magnetic properties. With that, a PF-based system with a high filler grade should be chosen to improve magnetic properties in thermoset-based systems. This choice goes along with a thermoset building a secondary product in the curing process and reacting at a lower temperature and time relative to EP. The lower tendency to build cross-linking junctions in PF after the network structure, according to [18], improves orientation even with a slightly higher viscosity in PF compared to EP. With that, the low tendency of adhesive forces between the fillers and the matrix material can exceed the lack of a low viscosity to some extent.

## 5. Conclusions

This paper showed the impact of the material system on the orientation and the magnetic properties in thermoset-based systems and multipolar bonded ring magnets considering two matrix materials and a changing filler grade. It was shown that the network structure and the reaction mechanism strongly affect the orientation of hard magnetic fillers and magnetic properties. With an increasing filler grade, the magnetic properties reach about 83% of the ideal value of a filler grade of 55 vol.-%. This goes along with a stack accumulation. Further, the sample depth, in which a proper orientation can take place, is limited due to the reduced outer magnetic field strength of the high tool temperature. The orientation of the fillers along the sample depth was correlated with the change of the magnetic properties along the characteristic pole  $D$ , reaching a plateau until about 8 mm from the outer diameter. This is similar to the results of the orientation, where a proper preferred direction along the fillers can only be reached 7 mm from the outer diameter. The reduction of the magnetic properties towards the inner diameter goes along with the reduction of the orientation grade. Therefore, the construction of a thermoset-based multipolar bonded magnet should be based on a PF material system with a high filler grade to increase the magnetic properties. The sample depth should be as low as possible with respect to the reduction of the outer magnetic field strength. Further, a final magnetisation has to be integrated within the production process of the sample.

In addition, investigations will be carried out on the impact of different process parameters to evaluate the possibility of improving the magnetic properties of the process conditions.

**Author Contributions:** U.R.: Conceptualisation, methodology, validation, investigation, writing—original draft preparation, visualisation; D.D.: writing—review and editing, supervision, project administration, funding acquisition. All authors have read and agreed to the published version of the manuscript.

**Funding:** This research was funded by the German Research Foundation (DFG) within the project DFG DR 412/36-1 “Duroplastgebundene spritzgegossene Dauermagneten mit definierter Magnetisierungsstruktur”. We acknowledge financial support by Deutsche Forschungsgemeinschaft and Friedrich-Alexander-Universität Erlangen-Nürnberg within the funding programme “Open Access Publication Funding”.

**Institutional Review Board Statement:** Not applicable.

**Informed Consent Statement:** Not applicable.

**Data Availability Statement:** Restrictions apply to the availability of these data. Data are available with the permission of the author.

**Acknowledgments:** We want to thank the German Research Foundation (DFG) for funding the project DFG DR 421/36-1 “Duroplastgebundene spritzgegossene Dauermagneten mit definierter Magnetisierungsstruktur” as well as Friedrich-Alexander-Universität Erlangen-Nürnberg for the funding programme “Open Access Publication Funding”.

**Conflicts of Interest:** The authors declare no conflict of interest. The funders had no role in the design of the study; in the collection, analyses or interpretation of data; in the writing of the manuscript or in the decision to publish the results.

## References

1. Cassing, W.; Kuntze, K.; Ross, G. *Dauermagnete: Mess- und Magnetisierungstechnik*, 3rd ed.; Expert-Verlag: Renningen, Germany, 2018.
2. Reppel, G.W. Duroplastgepresste Magnete—Werkstoffe, Verfahren und Eigenschaften. In *Kunststoffgebundene Dauermagnete: Werkstoffe, Fertigungsverfahren und Eigenschaften*; Ehrenstein, G.W., Drummer, D., Eds.; Springer VDI Verlag: Düsseldorf, Germany, 2004; pp. 14–36.
3. Drummer, D. Verarbeitung und Eigenschaften Kunststoffgebundener Dauermagnete. Ph.D. Thesis, Friedrich-Alexander-University, Erlangen, Germany, 2004.
4. Kurth, K.H.; Drummer, D. Influences on the Magnetic Properties of Injection Molded Multipolar Rings. *Int. Polym. Process.* **2016**, *31*, 356–363. [\[CrossRef\]](#)
5. Kurth, K. Zum Spritzgießen Polorientierter Kunststoffgebundener Dauermagnete. Ph.D. Thesis, Friedrich-Alexander-Universität Erlangen-Nürnberg, Erlangen, Germany, 2019.
6. Hagemann, B. Kunststoffgebundene Magnete in der Antriebstechnik—Möglichkeiten und Grenzen. In *Kunststoffgebundene Dauermagnete*; Springer VDI Verlag: Düsseldorf, Germany, 2004.
7. Altmann, N.; Halley, P.J.; Cooper-White, J.; Lange, J. The effects of silica fillers on the gelation and vitrification of highly filled epoxy-amine thermosets. *Macromol. Symp.* **2001**, *169*, 171–177. [\[CrossRef\]](#)
8. Bae, J.; Jang, J.; Yoon, S.-H. Cure Behavior of the Liquid-crystalline Epoxy/Carbon Nanotube System and the Effect of surface treatment of carbon fillers on cure reaction. *Macromol. Chem. Phys.* **2002**, *203*, 2196–2204. [\[CrossRef\]](#)
9. Dutta, A.; Ryan, M. Effect of fillers on kinetics of epoxy cure. *J. Appl. Polym. Sci.* **1979**, *24*, 635–649. [\[CrossRef\]](#)
10. Wang, X.; Jin, J.; Song, M.; Lin, Y. Effect of graphene oxide sheet size on the curing kinetics and thermal stability of epoxy resins. *Mater. Res. Express* **2016**, *3*, 105303. [\[CrossRef\]](#)
11. Halley, P.J. A new chemorheological analysis of highly filled thermosets used in integrated circuit packaging. *J. Appl. Polym. Sci.* **1997**, *64*, 95–106. [\[CrossRef\]](#)
12. Altmann, N.; Halley, P.J. The effect of fillers on the chemorheology of highly filled epoxy resin: I. Effects on cure transitions and kinetics. *Polym. Int.* **2003**, *52*, 113–119. [\[CrossRef\]](#)
13. Zhao, Z.; Zhanyu, Z.; Drummer, D. Thermal conductivity of aluminosilicate and aluminium oxide filled thermosets for injection molding. *Polymers* **2018**, *10*, 457. [\[CrossRef\]](#) [\[PubMed\]](#)
14. Zhao, Y.; Drummer, D. Influence of filler content and filler size on the curing kinetics of an epoxy resin. *Polymers* **2019**, *11*, 1797. [\[CrossRef\]](#) [\[PubMed\]](#)
15. Yushanov, S.P.; Isayev, A.I.; Levin, V.Y. Percolation simulation of the network degradation during ultrasonic devulcanization. *J. Polym. Sci. Part B Polym. Phys.* **1996**, *34*, 2409–2418. [\[CrossRef\]](#)
16. Maenz, T. Spritzgießtechnische Herstellung Duroplastgebundener Dauermagnete. Ph. D. Thesis, Technical University Chemnitz, Chemnitz, Germany, 2018.
17. Rösel, U.; Drummer, D. Correlation between the Flow and Curing Behavior of Hard Magnetic Fillers in Thermosets and the Magnetic Properties. *Magnetism* **2021**, *1*, 37–57. [\[CrossRef\]](#)
18. Rösel, U.; Drummer, D. Understanding the effect of material parameters on the processability of injection-molded thermoset-based bonded magnets. *Magnetism* **2022**, *2*, 211–228. [\[CrossRef\]](#)
19. Baur, E.; Brinkmann, S.; Osswald, T.; Rudolph, N.; Schmachtenberg, E. *Saechtling Kunststoff Taschenbuch*, 31st ed.; Carl Hanser Verlag: München, Germany, 2013.
20. Becker, G.W.; Braun, D. (Eds.) *Kunststoff Handbuch: Duroplaste*, 2nd ed.; Hanser: München, Germany, 1988.
21. Normenausschuß Kunststoffe (FNK) im DIN Deutsches Institut für Normung e.V. *Reaktionsharze, Reaktionsmittel und Reaktionsharzmassen*; Beuth Verlag GmbH: Berlin, Germany, 1989. Available online: <https://webstore.ansi.org/standards/din/din169451989de> (accessed on 12 April 2022).
22. Lechner, M.D.; Gehrke, K.; Nordmeier, E.H. *Makromolekulare Chemie*; Birkhäuser: Basel, Switzerland, 2003.
23. Ormerod, J.; Constantinides, S. Bonded permanent magnets: Current status and future opportunities (invited). *J. Appl. Phys.* **1997**, *81*, 4816–4820. [\[CrossRef\]](#)
24. Hering, E.; Martin, R.; Stohrer, M. *Physik für Ingenieure*, 12th ed.; Springer: Berlin/Heidelberg, Germany, 2016.
25. Johannaber, F.; Michaeli, W. *Handbuch Spritzgießen*, 2nd ed.; Hanser: München, Germany, 2004.

- 
26. *DIN EN ISO 11357-1:2016*; Kunststoffe-Dynamische Differenz Thermoanalyse (DSC)-Teil 1: Allgemeine Grundlagen. Deutsches Institut für Normung e. V.: Berlin, Germany, 2016.
  27. *DIN EN ISO 53019-1:2008*; Viskosimetrie-Messung von Viskositäten und Fließkurven mit Rotationsviskosimetern-Teil 1: Grundlagen und Messgeometrie. Deutsches Institut für Normung e. V.: Berlin, Germany, 2008.

**Disclaimer/Publisher's Note:** The statements, opinions and data contained in all publications are solely those of the individual author(s) and contributor(s) and not of MDPI and/or the editor(s). MDPI and/or the editor(s) disclaim responsibility for any injury to people or property resulting from any ideas, methods, instructions or products referred to in the content.